Published in final edited form as:
Cornea. 2015 April ; 34(4): 464–470. doi:10.1097/ICO.0000000000000369.

In vivo confocal microscopic analysis of normal human anterior limbal stroma

Saumi Mathews, M.Sc, M.Phil[*], **Jaya Devi Chidambaram, MD, MRCOph**[†,‡], **Shruti Lanjewar, MS**[‡], **Jeena Mascarenhas, MS**[‡], **Namperumalsamy Venkatesh Prajna, DNB, FRCOph**[‡], **Veerappan Muthukkaruppan, Ph.D**[§], and **Gowri Priya Chidambaranathan, Ph.D.**[*]

[*]Department of Immunology and Stem Cell Biology, Aravind Medical Research Foundation, Madurai

[†]International Centre for Eye Health, London School of Hygiene and Tropical Medicine, Keppel Street, London WC1E 7HT, UK

[‡]Department of Cornea, Aravind Eye Hospital and Postgraduate Institute of Ophthalmology, Madurai

[§]Advisor-Research, Aravind Medical Research Foundation, Madurai

Abstract

Purpose—To characterize the microarchitecture of the anterior limbal stroma in healthy individuals using *in vivo* confocal microscopy (IVCM) and to correlate it with mesenchymal stem cells (MSCs), a component of the limbal-niche.

Methods—The corneal side of the superior limbus was scanned in 30 eyes of 17 normal subjects beyond the basal epithelium, deep into the stroma using a HRT III laser scanning microscope. The IVCM findings were correlated with the immunohistochemical features of MSCs in the anterior limbal stroma.

Results—Clusters of hyperreflective structures were observed in the anterior limbal stroma, subjacent to the basal epithelium (depth: 50.2±8.7 - 98±12.8 μm), but not in the corneal stroma. The structures showed unique morphology compared to epithelial cells, keratocytes, neurons and dendritic cells. In parallel, confocal analysis of immunostained sections showed clusters of cells, double positive for MSC specific markers (CD90 and CD105) in the anterior limbal stroma at a depth of 55.3±12.7 μm to 72±37.6 μm. The organization and distribution of the MSC clusters locates them within the hyperreflective region in the anterior limbal stroma.

Conclusions—The hyperreflective structures, demonstrated for the first time in the human anterior limbal stroma, probably represent an important component of the limbal-niche. Our approach of *in vivo* imaging may pave the way for assessing the limbal stromal health.

Corresponding Author: Dr. Gowri Priya Chidambaranathan, Scientist Gr. II, Department of Immunology and Stem Cell Biology, Aravind Medical Research Foundation, Dr. G Venkataswamy Eye Research Institute, No.1, Anna Nagar, Madurai – 625 020 Tamil Nadu, India. gowri@aravind.org, Telephone: 91-452-4356550; Fax: 91-452-2530984.

Disclosure: M.Saumi, None; C. Jaya Devi, None; L Shruti, None; M. Jeena, None; C. Gowri Priya, None; N.V. Prajna, None; V. Muthukkaruppan, None.

Europe PMC Funders Author Manuscripts

Keywords

Limbal stromal niche; MSCs; IVCM; Hyperreflective region

Introduction

Stem cells of the corneal epithelium reside in the basal limbal layer at the corneo-scleral junction. Dysfunction or deficiency of these limbal epithelial stem cells (LESCs) either due to inherited (aniridia, congenital erythrokeratodermia) or acquired (thermal/chemical injury or chronic inflammatory) diseases disrupts corneal epithelial homeostasis, leading to conjunctivalization, neovascularization and eventually to blindness. This condition is known as limbal stem cell deficiency (LSCD). In the past, LSCD diagnosis rested primarily on history and clinical signs[1], with confirmation by histology[2] and impression cytology.[3] With the advent of *in vivo* laser scanning confocal microscopy (IVCM), live imaging of the corneo-limbal epithelial architecture in healthy individuals[4-7] and LSCD patients[2,3,8] became possible. Confirmation of loss of palisades of Vogt (POV) and conjunctivalization by IVCM is now an adjuvant to diagnose LSCD.

IVCM scanning in the above studies focused on the POV[2-8] in the limbus, but not the microarchitecture of the limbal stroma. Recent studies using human cadaver tissue examined the cellular components of the anterior limbal stroma and their role in the maintenance of stemness in the basal epithelium.[9-12] However, the structure and function of the anterior limbal stroma has not been studied *in vivo* in normal individuals or patients with LSCD. Hence the former is the objective of the present study using IVCM.

Material and Methods

In vivo confocal microscopic analysis of limbus and cornea in healthy individuals

Study Subjects—Normal subjects with prominent POV in the superior limbus as observed under slit lamp biomicroscopy were recruited. The exclusion criteria were a history of ocular trauma, prior eye surgery, contact lens wear, ocular or systemic disease that might affect the cornea and limbus. A total of 30 eyes of 17 healthy subjects (7 males; 10 females) were studied after obtaining their written informed consent. The median age of healthy subjects recruited for the study was 30 years (range 24-62 years). The research adhered to the tenets of the Declaration of Helsinki and the study was approved by the Institutional Ethical Committee of Aravind Eye Care System.

IVCM examination—IVCM examination of central cornea and superior limbus was performed using the Heidelberg Retina Tomograph III (HRT III) with Rostock Corneal Module (RCM) (Heidelberg Engineering, Germany), after anesthetizing the eye with 0.5% proparacaine ophthalmic solution (Aurocaine, Aurolab, Madurai) as described earlier.[6] GenTeal gel (Novartis India Limited, Mumbai) was used as a coupling agent between the applanating lens cap (TomoCap, Heidelberg Engineering, Germany) and the HRTIII RCM. During acquisition of images, the subjects were instructed to focus on the instrument's red light fixation that was moved until the eye was in the imaging axis of RCM. The operator

manually moved the RCM objective lens until the first epithelial layer was in focus. For accurate measurements, pachymetry reading was set to zero at the image that captured the anterior-most epithelial cell layer. The two dimensional images comprised 384 × 384 pixels, with a 400 μm × 400 μm field of view. The motorized lens and digital camera of the IVCM automatically captured an image stack, called a volume scan, consisting of 40 consecutive images taken with 2 μm between each image. A minimum of five volume scans were taken in several locations in the corneal side of the superior limbus, extending from the epithelium to the deepest stromal level at which structures could be resolved. In six eyes of healthy individuals, the scleral side of the limbus was also scanned similarly.

Analysis of IVCM images—The cell density of basal and wing cells of corneal and limbal epithelium was measured using the IVCM Heidelberg Eye Explorer software (Heidelberg Engineering, Germany) in manual cell count processing mode. A mean cell density was calculated from the three best in focus frames of each layer examined. The cell diameter was measured using ImageJ software (National Institute of Health, Maryland, USA). The depth at which various types of cells occur in limbus and cornea was estimated by two independent observers (GPC, SM) using the IVCM pachymetry. A minimum of three scans were used for each eye and a mean value was calculated.

Confocal microscopic analysis of immunostained cadaver corneo-limbal tissues

Samples—Human tissues were handled according to the tenets of the Declaration of Helsinki. Fresh enucleated cadaver globes of donors below 75 years of age, without any evidence of trauma or surgery were procured within six hours of death from the Rotary Aravind International Eye Bank at Aravind Eye Hospital, Madurai.[13]

Histology and immunostaining—Tangential sections of paraffin embedded corneo-limbal tissues from three different donors were stained with haematoxylin-eosin following standard methods. For immunostaining, serial 5 μm cryosections of corneo-limbal tissues were processed as described earlier.[13] The primary antibodies used were Thy 1 mouse monoclonal IgG_1 (CD 90) or endoglin mouse monoclonal IgG_1 (CD 105).

Confocal microscopy—Fluorescence *z* stack images were acquired using confocal microscope (Leica AOBS-TCS SP2, Heidelberg, Germany) as described previously.[13] In order to distinguish between Alexa 633 and PI, false color (blue) was given to PI stained nuclei.

Statistics—Mean and standard deviation (SD) were calculated. Non-parametric Mann-Whitney U test was applied for comparing two variables (Stata Ver 11.0, Stata College Station, TX). A value of $p < 0.05$ was considered significant.

Results

IVCM analysis

The central cornea from epithelium to endothelium (Figure 1 A-G) and the superior limbus from epithelium to stroma (Figure 1 H-N) were scanned.

Organization of the Cornea—The superficial epithelial cells appeared polygonal with bright cytoplasm and nucleus with perinuclear dark halo (Figure 1A). The wing cells (Figure 1B) in the suprabasal layers (18.3 ± 5.0 μm thick) and cells (Figure 1C) in the basal layer (12.7 ± 3.8 μm thick) appeared dark with well-demarcated highly reflective cell borders. The sub-basal nerve plexus was characterized by linear, branching hyperreflective nerve fibers. Bowman's layer (Figure 1D) was observed at a mean depth of 46.8 (±7.4μm) from the surface epithelium. The keratocytes in the corneal stroma (from 48 to 622 μm) had bright oval nuclei with transparent cell bodies and the connecting lamellae appeared dark (Figure 1E). The Descemet's membrane was thin without cells (Figure 1F). The endothelium appeared as a layer of uniform hexagonal cells arranged in a honey-comb pattern (Figure 1G).

Organization of the Limbus

Limbal epithelial architecture: Sequential scanning of the limbus (corneal side) from suprabasal epithelium deep into the stroma is shown for one subject (Figure 2). The wing cells in the suprabasal layer of limbus (27.0 ± 14.2 μm thick) were similar to those seen in the cornea with highly reflective well-demarcated cell borders and dark intracellular regions (Figure 1I, 2A). In contrast, the basal cells in the limbal palisades of Vogt (39.9 ± 16.6 μm thick) were hyperreflective with indistinguishable borders (Figure 1J, K, 2B). Morphometric analysis revealed that these cells were significantly smaller in size than corneal basal epithelial cells (Table 1). Dendritic cells with their bright cell body and processes were observed as a layer immediately beneath the epithelial cells (Figure 1K, 2C).

Limbal stromal architecture: Clusters of hyperreflective structures were seen at a mean depth of 50.2 ± 8.7 μm in the anterior limbal stroma subjacent to basal epithelium (Figure 2C). These individual clusters extended posteriorly (up to 98 ± 12.8 μm) to form a continuous non-homogenous structure with varying intensities of brightness (Figure 1L). At the deeper level, they were seen surrounding the blood vessels, which appeared as dark streaks at a depth of 60.0 ± 8.4 μm (Figure 1M, 2D, E). While imaging, bright moving blood cells were seen within the dark streaks. The hyperreflective structures were also observed in the interpalisade regions, extending from the clusters in the anterior stroma. They formed continuous hyperreflective linear strands, lined by the basal epithelial cells (Figure 3). In the subsequent confocal images of the stroma (up to 158 μm), keratocytes with bright nuclei were observed (Figure 1N, 2F). The above findings were confirmed in the oblique sections through the stroma of cornea (Figure 4A) and limbus (Figure 4B). The hyperreflective structures were observed in the corneal side of limbus in all 30 eyes.

The anterior limbal stroma at the scleral side of POV was scanned in six eyes. Hyperreflective linear strands were observed between the rete pegs, lined by bright limbal basal epithelial cells (Supplementary Figure 1A). At a deeper level, the stroma below the rete pegs appeared totally hyperreflective, alternating with dark areas corresponding to the interpalisade region (Supplementary Figure 1B). In contrast to the cluster of hyperreflective structures seen in the corneal side of limbus, the stromal hyperreflection in the scleral side was homogenous. Keratocytes were not seen in this region.

Identification of MSCs in anterior limbal stroma

Hematoxylin-eosin stained tangential sections of cadaver limbus were used to examine the cellular organization in the limbal stroma. A large number of individual cells and highly compact clusters were observed in the anterior stroma, extending into the interpalisade region (Figure 5). Confocal microscopic analysis of tangential sections, immunostained for MSC specific markers revealed the presence of clusters of cells double positive for CD90 and CD105 in the anterior limbal stroma at the corneal side (Figure 6A). Similar clusters were not observed in the corneal stroma. This was confirmed by observing several sequential images of the cornea (data not shown). The location of CD90 and CD105 positive cells corresponded to the hyperreflective clusters in IVCM images subjacent to the basal limbal epithelium (Figure 6). The hyperreflective structures, located subjacent to the limbal basal epithelium and between the interpalisade ridges were identical to the clusters of MSCs.

A composite picture was prepared using IVCM scans at six successive regions from the peripheral cornea to sclera, at the horizontal and vertical levels (Supplementary Figure 2). This demonstrated the extensive distribution of the hyperreflective structures in the anterior limbal stroma (Supplementary Figure 2B b4, 5; c1-5, d3-5). Based on the distribution of CD90, CD105 double positive cells, the width of the region containing clusters of cells was found to be 1.42-1.52 mm.

Discussion

In vivo confocal microscopy has gained prominence in Ophthalmology as a non-invasive tool to image the cornea from epithelium to endothelium in healthy eyes and in pathological conditions including corneal dystrophies, keratoconus, iridocorneal endothelial syndrome as well as infectious keratitis due to acanthamoeba, fungi and herpes virus.[14-16] It has also produced live images of the corneal and limbal epithelial architecture in LSCD (Table 2). Confocal microscopy can also document the progressive changes in POV in patients with different grades of aniridia-related keratopathy.[17]

Our IVCM analysis of the corneal and limbal epithelium (Figure 1, Table 1) confirmed earlier reports on the cell size and density.[5,6] Our study added data regarding the thickness of the corneal and limbal epithelial layers (Table 1).

Earlier studies limited the use of IVCM to examine POV in healthy individuals and LSCD patients. There is no detailed IVCM study of the limbal stroma, except for a brief report by Kobayashi and Sugiyama (2005).[4] In the present study, we carried out IVCM analysis of the limbus, beyond the basal epithelium to the deepest stromal level at which structures could be resolved. The presence of unique hyperreflective clusters subjacent to the limbal basal epithelium were observed in the anterior limbal stroma and surrounding blood vessels at deeper layers (Figure 2). Similar non-homogenous hyperreflective structures can be seen in the limbal stroma towards the corneal side in the montage pictures in earlier reports[5,6]; however, they were not described. Similarly, the stromal cords in between the basal epithelium of POV as reported by others [6,7,18] are comparable to the hyperreflective linear strands, described in the present study (Figure 3).

Hematoxylin-eosin stained tangential sections (Figure 5) revealed a large number of stromal cells either as clusters or as individual cells in the anterior limbal stroma adjacent to the basal epithelium. Other researchers similarly described high cellularity in the anterior limbal stroma in phalloidin green and propidium iodide stained confocal sections.[19] The cellular components in this region include (i) ABCG2 and PAX6 positive multipotent stromal stem cells,[20] (ii) vimentin positive mesenchymal cells, expressing ESC markers[9], and (iii) CD34, CD31, Flk-1,VWF positive stromal cells.[12] In another study, we demonstrated the presence of clusters of CD90 and CD105 positive MSCs in the native anterior limbal stroma, along with vimentin positive mature keratocytes distributed singly (unpublished data). Immunohistochemical analysis of tangential sections of limbal tissues revealed the profile, location and distribution of the CD90 and CD105 positive cells at different depths of anterior limbal stroma (Figure 6).

The precise mechanism, causing hyperreflection in the anterior limbal stroma on IVCM is not clear. Image formation is based on the number, size and orientation of the organelles or particles scattering light. The CD90 and CD105 positive cells, which were observed as clusters of closely packed cells in the anterior limbal stroma subjacent to basal epithelial cells (Figure 6A,E), may form the hyperreflective clusters just posterior to the bright basal epithelium. Other factors that scatter light in that region include, keratocytes as well as the unique extracellular matrix. The hyperreflection is not an artifact as it was possible to identify keratocytes with normal appearance beyond this region. Thus, the hyperreflective structures and clusters of MSCs were found similar in terms of their location, organization and distribution in the anterior limbal stroma and the POV (Figure 6).

The anterior limbal stroma is responsible to maintain stemness in the limbal basal epithelium.[9,10] MSCs in the limbal stroma are more primitive than those in corneal stroma and support LESCs, demonstrating that these stromal stem cells constitute a component of the limbal-niche (unpublished data). Therefore, it is possible that the hyperreflective structures on IVCM represent the limbal stromal niche. Studies on patients with LSCD will shed additional data on the role of these structures in pathologic states.

In conclusion, we demonstrate that the previously undescribed hyperreflective structures in the anterior limbal stroma, probably represent an important component of the limbal-niche.

Supplementary Material

Refer to Web version on PubMed Central for supplementary material.

Acknowledgements

This study was supported by Defence Research and Development Organization (DRDO), India, (DLS/81/4822/LSRB-227/SHDD/2010), Wellcome Trust, UK, (Grant no. 09747/Z/11/Z), and AMRF –Aurolab Research Grant. The authors thank Dr. Ken Bassett, Professor, The University of British Columbia, for editing the manuscript; Mr. D. Saravanan, Manager, Rotary Aravind International Eye Bank, for helping in getting the cadaver tissues within the stipulated time; Mrs. Sumithra Subbaiah Rangasamy, Cornea Clinic, Aravind Eye Hospital, Madurai, for technical help.

Grant: Supported by Defence Research and Development Organization (DRDO), India (DLS/81/4822/LSRB-227/SHDD/2010); Wellcome Trust UK (Grant no. 097437/Z/11/Z); AMRF –Aurolab Research Grant, India.

References

1. Dua HS, Saini JS, Azuara-Blanco A, et al. Limbal stem cell deficiency: concept, aetiology, clinical presentation, diagnosis and management. Indian J Ophthalmol. 2000; 48:83e92. [PubMed: 11116520]
2. Miri A, Alomar T, Nubile M, et al. In vivo confocal microscopic findings in patients with limbal stem cell deficiency. Br J Ophthalmol. 2012; 96:523–9. [PubMed: 22328810]
3. Nubile M, Lanzini M, Miri A, et al. In vivo confocal microscopy in diagnosis of limbal stem cell deficiency. Am J Ophthalmol. 2013; 155:220–32. [PubMed: 23127748]
4. Kobayashi A, Sugiyama K. In vivo corneal confocal microscopic findings of palisades of Vogt and its underlying limbal stroma. Cornea. 2005; 24:435–7. [PubMed: 15829801]
5. Patel DV, Sherwin T, McGhee CN. Laser scanning in vivo confocal microscopy of the normal human corneoscleral limbus. Invest Ophthalmol Vis Sci. 2006; 47:2823–7. [PubMed: 16799020]
6. Miri A, Al-Aqaba M, Otri AM, et al. In vivo confocal microscopic features of normal limbus. Br J Ophthalmol. 2012; 96:530–6. [PubMed: 22328815]
7. Zarei-Ghanavati S, Ramirez-Miranda A, Deng SX. Limbal lacuna: a novel limbal structure detected by in vivo laser scanning confocal microscopy. Ophthalmic Surg Lasers Imaging. 2011; 42:e129–31. Online. [PubMed: 22150603]
8. Deng SX, Sejpal KD, Tang Q, et al. Characterization of limbal stem cell deficiency by in vivo laser scanning confocal microscopy: a microstructural approach. Arch Ophthalmol. 2012; 130:440–5. [PubMed: 22159172]
9. Chen SY, Hayashida Y, Chen MY, et al. A new isolation method of human limbal progenitor cells by maintaining close association with their niche cells. Tissue Eng Part C Methods. 2011; 17:537–48. [PubMed: 21175372]
10. González S, Deng SX. Presence of native limbal stromal cells increases the expansion efficiency of limbal stem/progenitor cells in culture. Exp Eye Res. 2013; 116:169–76. [PubMed: 24016868]
11. Lim MN, Hussin NH, Othman A, et al. Ex vivo expanded SSEA-4+ human limbal stromal cells are multipotent and do not express other embryonic stem cell markers. Mol Vis. 2012; 18:1289–300. [PubMed: 22665977]
12. Li GG, Zhu YT, Xie HT, et al. Mesenchymal stem cells derived from human limbal niche cells. Invest Ophthalmol Vis Sci. 2012; 53:5686–97. [PubMed: 22836771]
13. Arpitha P, Prajna NV, Srinivasan M, et al. High expression of p63 combined with a large N/C ratio defines a subset of human limbal epithelial cells: implications on epithelial stem cells. Invest Ophthalmol Vis Sci. 2005; 46:3631–6. [PubMed: 16186343]
14. Guthoff RF, Zhivov A, Stachs O. In vivo confocal microscopy, an inner vision of the cornea-a major review. Clin Experiment Ophthalmol. 2009; 37:100–17. [PubMed: 19338608]
15. Kobayashi A, Yokogawa H, Sugiyama K. In Vivo biopsy of the human cornea. In: Neil Lagali, ed. In confocal laser microscopy -principles and applications in medicine, biology, and the food sciences. InTech Janeza Trdine, Rijeka, Croatia. 2013; 39:49.
16. Villani E, Baudouin C, Efron N, et al. In vivo confocal microscopy of the ocular surface: from bench to bedside. Curr Eye Res. 2014; 39:213–31. [PubMed: 24215436]
17. Lagali N, Edén U, Utheim TP, et al. In vivo morphology of the limbal palisades of vogt correlates with progressive stem cell deficiency in aniridia-related keratopathy. Invest Ophthalmol Vis Sci. 2013; 54:5333–42. [PubMed: 23860752]
18. Zheng T, Xu J. Age-related changes of human limbus on in vivo confocal microscopy. Cornea. 2008; 27:782–6. [PubMed: 18650663]
19. Shortt AJ, Secker GA, Munro PM, et al. Characterization of the limbal epithelial stem cell niche: novel imaging techniques permit in vivo observation and targeted biopsy of limbal epithelial stem cells. Stem Cells. 2007; 25:1402–9. [PubMed: 17332511]
20. Du Y, Funderburgh ML, Mann MM, et al. Multipotent stem cells in human corneal stroma. Stem Cells. 2005; 23:1266–75. [PubMed: 16051989]

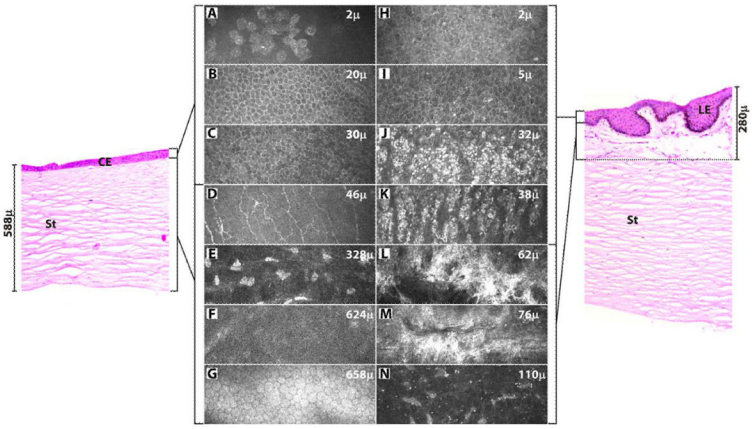

FIGURE 1. ***In vivo*** **confocal images of cornea (A-G) and limbus (H-N) of a normal human subject in comparison to vertical meridian sections of cadaver corneal (left) and limbal (right panel) tissues, stained for hematoxylin-eosin**

The cornea was scanned from epithelium to endothelium and limbus from epithelium to deepest stroma (110 μm) at which structures could be resolved (n = 30 eyes). A, H - superficial epithelium; B, I - suprabasal layer; C, J, K - basal layer; D - Bowman's layer with nerve plexus; E, N - stroma with keratocytes; F - Descemet's membrane; G - endothelium; L - anterior stroma with hyperreflective region; M - hyperreflective region surrounding a blood vessel; CE - corneal epithelium; LE - limbal epithelium; St - stroma.

Europe PMC Funders Author Manuscripts

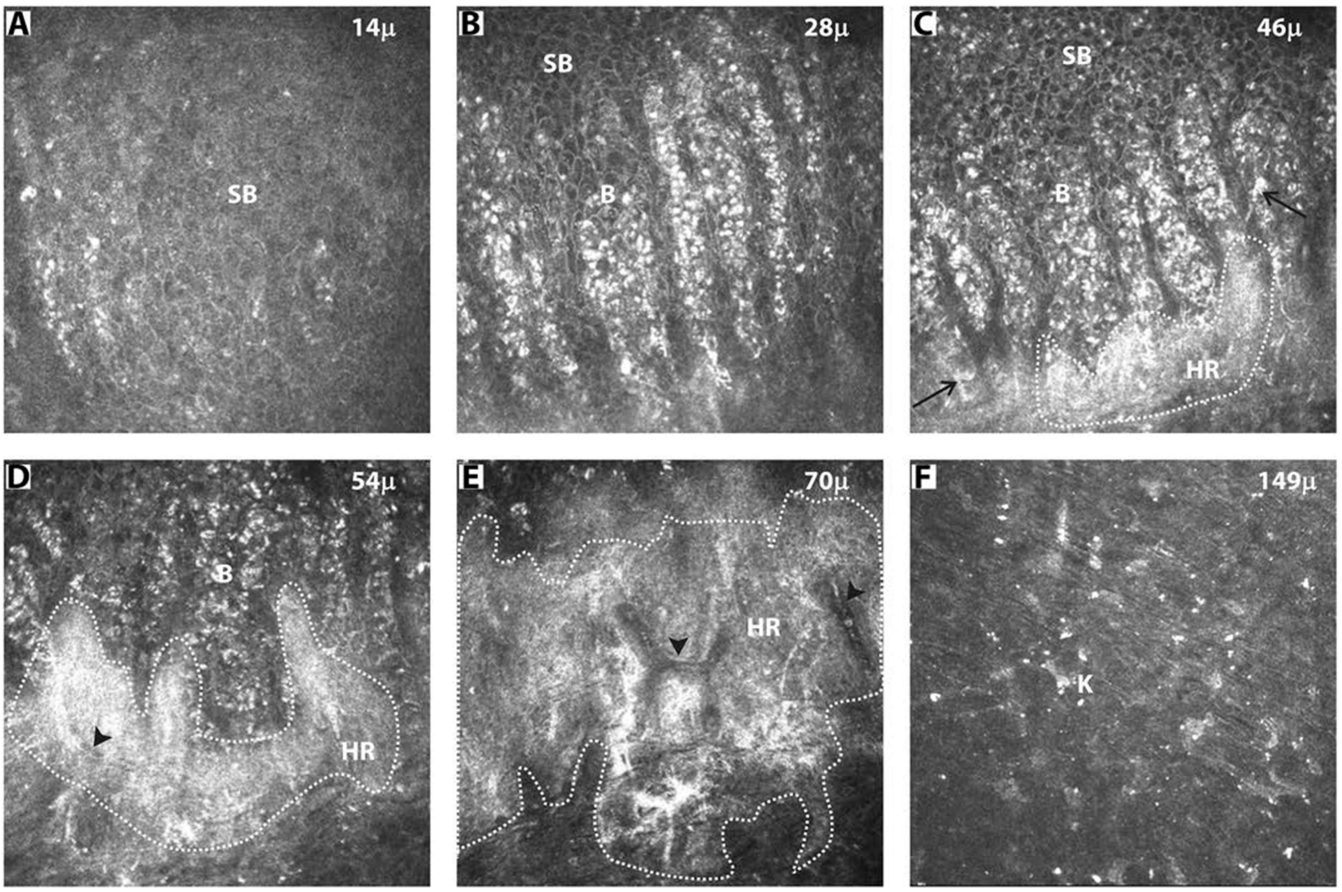

FIGURE 2. Sequential *in vivo* confocal images of superior limbus (corneal side) of a healthy subject

(A) suprabasal cells; (B) basal cells; (C) hyperreflective structures (HR) in the anterior limbal stroma subjacent to the basal cells and dendritic cells (arrow); (D, E) continuous HR surrounding the blood vessels (arrow head); (F) Keratocytes (K) in deeper stroma; SB - suprabasal epithelial cells; B – basal epithelial cells. All images are 400 × 400 μm, n = 30 eyes.

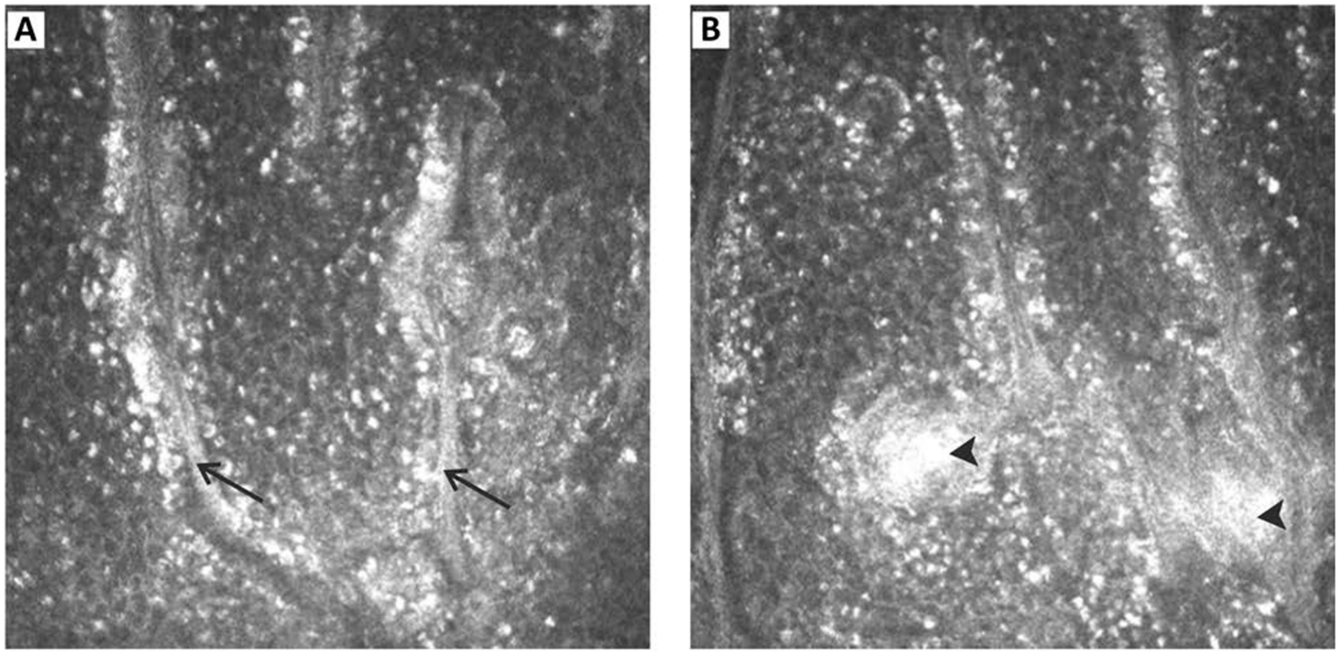

FIGURE 3. IVCM images showing the presence of linear strands of hyperreflection in the interpalisade ridges

(arrow) lined with bright basal epithelial cells (A). In some regions, these bright linear structures extended into the rete pegs (arrow head) (B). All images are 400 × 400 μm, n = 30 eyes.

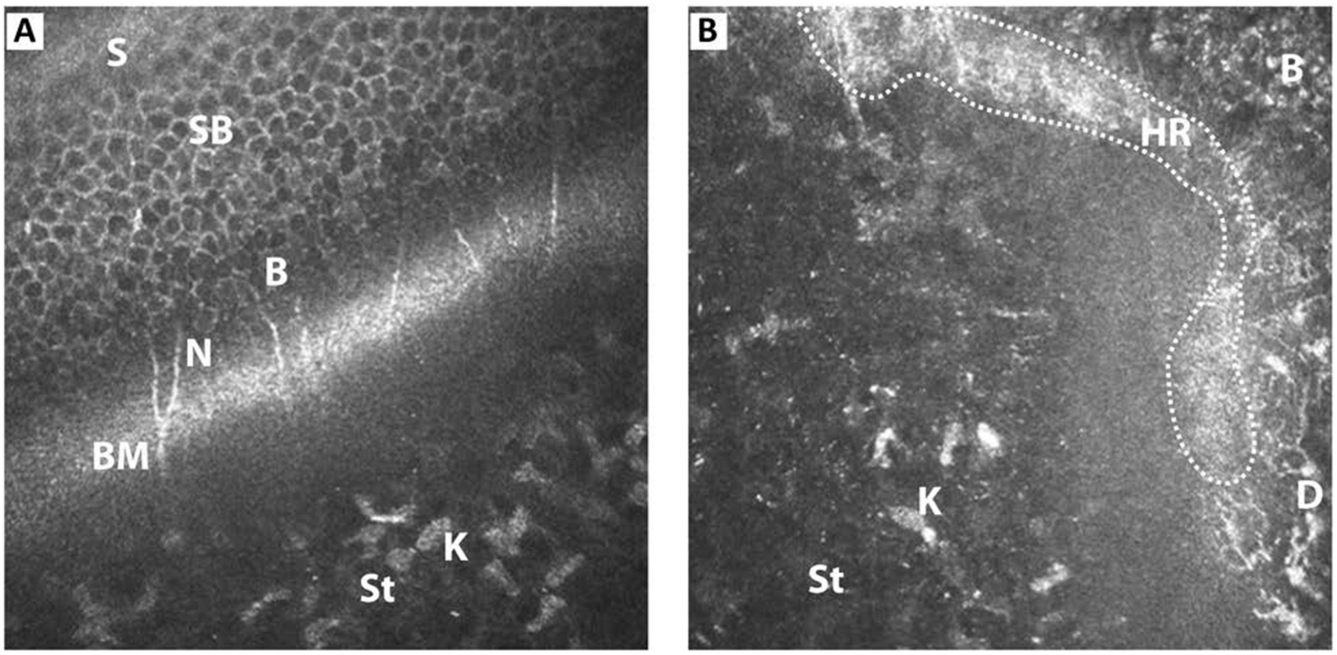

FIGURE 4. Oblique section of (A) corneal epithelium and (B) limbal epithelium through their anterior stroma, showing all layers

B - basal epithelium; BM - Bowman's layer; D - dendritic cells; K - keratocytes; N - nerve plexus; HR - hyperreflective region; S - superficial epithelium; SB - suprabasal epithelium; St - anterior stroma.

Europe PMC Funders Author Manuscripts

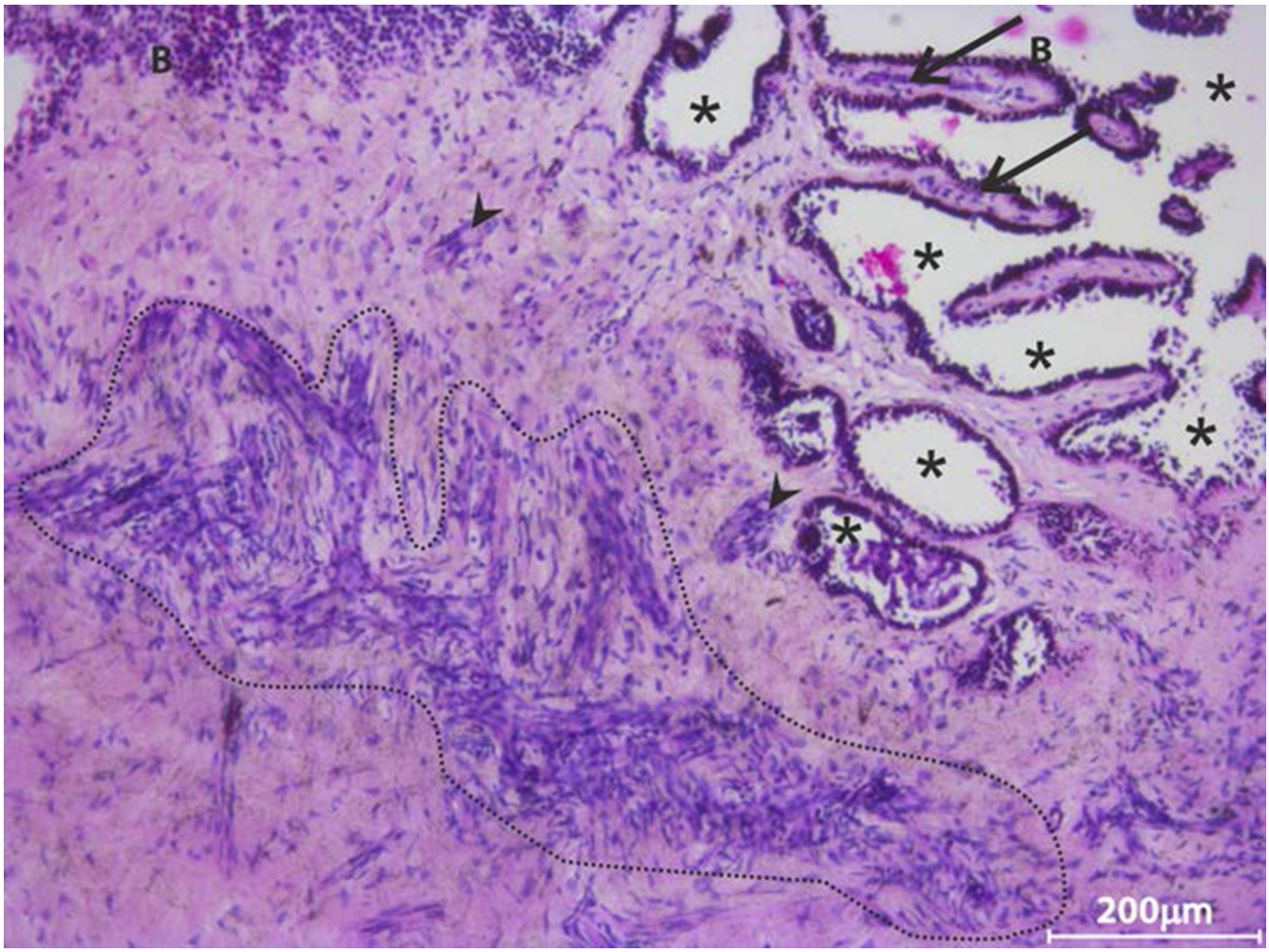

FIGURE 5. Representative haemotoxylin-eosin stained tangential limbal section

(n = 3 sections of different donor eyes) showing the presence of a large number of stromal cells either as clusters (highlighted region, arrow head) or as individual cells adjacent to basal epithelial cells. Such cell clusters were also observed in the interpalisade region (arrow). Location of * indicates the epithelial region wherein the epithelial cells might have been lost in the donor eye; B - basal epithelium.

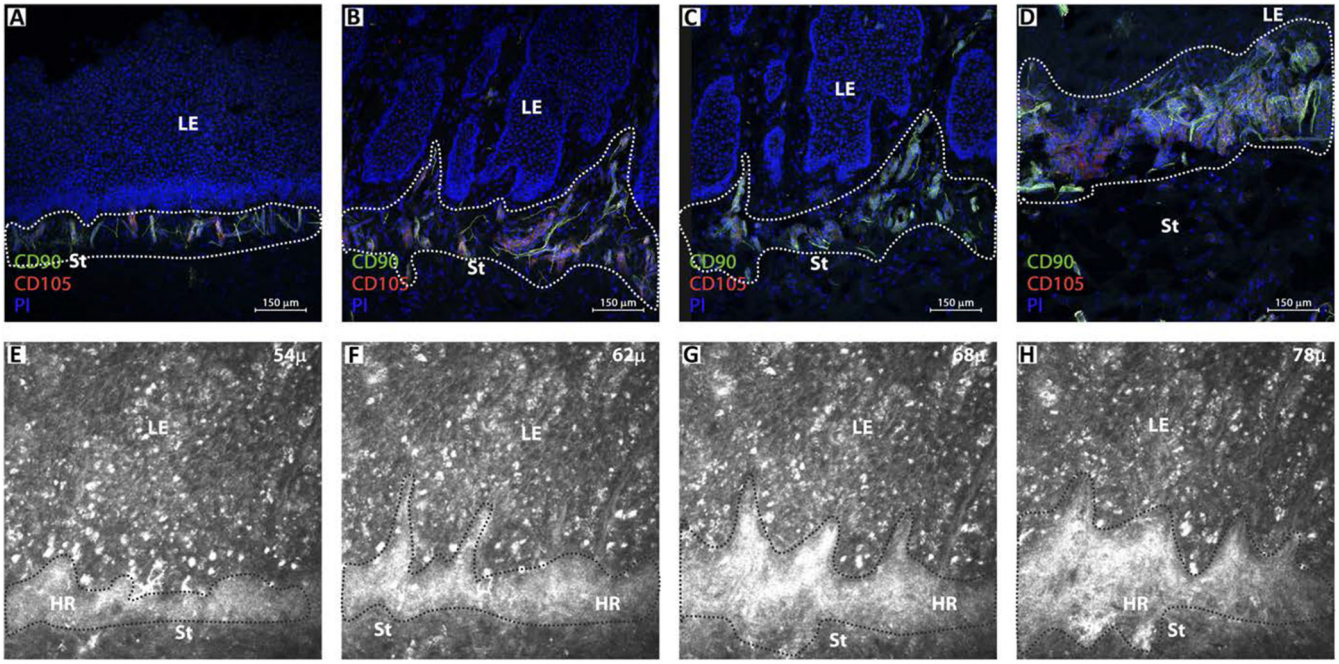

FIGURE 6. Comparison of sequential confocal microscopic images of immunostained [CD90-FITC(green); CD105-Alexa 633(red); propidium iodide (blue)] tangential sections of cadaver limbus (A-D) with *in vivo* confocal microscopic images of superior limbus in a healthy subject (E-H)

Based on the location and morphological features, the unique clusters of CD90 and CD105 positive mesenchymal stem cells observed in donor limbal sections appear as hyperreflective (HR) structures in the anterior limbal stroma by IVCM. A minimum of three different sections from each of the three donors were analyzed. LE - limbal epithelium; St - stroma. All IVCM images are 400 × 400 µm.

Europe PMC Funders Author Manuscripts

Europe PMC Funders Author Manuscripts

Table 1
Comparison of the morphometric data of corneal and limbal epithelium

	Corneal Epithelium			Limbal Epithelium		
	Cell density (cells/mm^2)	Cell diameter (μm)	Thickness (μm)	Cell density (cells/mm^2)	Cell diameter (μm)	Thickness (μm)
Suprabasal Layer	4078 ± 237	21.5 ± 1.3	18.3 ± 5.0	3790 ± 320	21.2 ± 1.2	27 ± 14.2
Basal Layer	6787 ± 274	12.8 ± 0.7	12.7 ± 3.8	7324 ± 220	10.6 ± 1.0*	39.9 ± 16.7†

The morphometric data of corneal and limbal epithelium of three subjects scanned are compared. The data are represented as mean ± SD.

* $p < 0.05$ compared to corneal basal epithelial cell diameter

† refers to the thickness of POV

Europe PMC Funders Author Manuscripts

Table 2

Summary of reports on IVCM analysis of limbus in healthy subjects and LSCD patients

Reference	IVCM used	No. eyes(subjects)		Major Finding	
		Healthy	LSCD	Limbal Epithelium	Limbal Stroma
Kobayashi & Sugiyama (2005)[4]	ConfoScan 2	4 (2)	-	Basal cells in POV significantly smaller than those of central cornea.	Spatter-like pattern, dark striae like structures in mid stroma.
Patel *et al.*, (2006)[5]	HRT II RCM	50 (50)	-	Significant decrease in the limbal basal epithelial cell density with age.	-
Zheng & Xu (2008)[18]	ConfoScan 3	160 (160)	-	Number of POV declined with age; age-related increase in size of limbal basal epithelial cells; Stromal cords in between basal epithelium of POV.	-
Zarei-Ghanavati *et al.*, (2011)[7]	HRT III RCM	2 (2)	2(2)	Lacuna-like structures with tightly packed limbal epithelial cells extending into stroma are lost in LSCD condition. Stromal cords in between basal epithelium of POV.	-
Deng *et al.*, (2012)[8]	HRT III RCM	12 (10)	27 (20)	In LSCD, the basal epithelial cells become metaplastic; decrease in basal epithelial density.	-
Miri *et al.*, (2012)[6]	HRT II RCM	46(29)	-	Epithelial cells in the limbal epithelial crypts significantly smaller and extend into the stroma at the conjunctival end of POV. Stromal cords in between basal epithelium of POV.	
Miri *et al.*, (2012)[2]	HRT II RCM	-	23 (17)	In LSCD, loss of limbal palisade architecture with cellular cystic changes and sub-epithelial fibrosis.	-
Nubile *et al.*, (2013)[3]	HRT II RCM	10 (10)	20 (17)	Demonstrated variable degree of alterations in LSCD – loss of POV, cystic epithelial changes and sub epithelial fibrosis; IVCM has high degree of concordance with impression cytology.	-
Current Study	HRT III RCM	30 (17)	-	Limbal basal epithelial cells smaller than those of central cornea. Depth at which various layers occur are indicated.	Unique clusters of hyper-reflective structures subjacent to limbal basal epithelium that formed a complete network deep in the anterior stroma; surrounding blood vessels. Such structures were absent in corneal stroma.

ConfoScan 2/3, Nidek Technologies, Vigonza, Italy; HRT II/III RCM - Heidelberg Retina Tomograph II/III Rostock Corneal Module (Heidelberg EngineeringGmBH, Dossenheim, Germany); LSCD-Limbal Stem Cell Deficiency; POV – Palisades of Vogt